First-principles study of the mechanism of ethylene epoxidation over Ag–Cu particles†

Simone Piccinin,[ab] Ngoc Linh Nguyen,[c] Catherine Stampfl[b] and Matthias Scheffler[d]

Received 16th June 2010, Accepted 15th September 2010
DOI: 10.1039/c0jm01916j

Silver–copper alloys have been proposed as catalysts for ethylene epoxidation due to their superior selectivity compared to pure silver, the predominant catalyst for this reaction. Under reaction conditions it has been previously shown that, rather than a two-dimensional (2D) Ag–Cu alloy, a thin copper oxide-like layer forms on top of silver, and several possible surface structures were identified (*Phys. Rev. Lett.*, 2010, **104**, 035503). By means of density-functional theory calculations, we study the mechanism of ethylene epoxidation catalyzed by the thin oxide-like surface structures. We identify different reaction pathways that will compete and/or synergetically interplay in the catalysis. In general, the reaction mechanism is structure-dependent and the reaction does not always proceed through the formation of (meta)stable intermediates, in contrast to clean Ag and the 2D alloy. Analyzing the competing reactions, we discuss how the addition of Cu improves the selectivity and stress the overall importance of accounting for the effect of ambient conditions.

I. Introduction

Transition metal particles of nanometer-scale dimensions are the active material in many industrial catalysts.[1] Obviously, the surface composition and structure of the catalysts plays a critical role, strongly influencing the catalyst performance.[1–3] It has been recognized that the conditions (temperature and partial pressures of the reactants) under which catalysts operate crucially influence their nanocrystalline shape, surface structure and the catalyst activity.[4,5] For instance, several metal catalysts, when operating in high temperature and high pressure regimes, *i.e.* in conditions typically encountered in industrial applications, can develop a thin oxide-like film at the surface.[6,7] The structure of these thin films can be significantly different from the stable surface structures typically found under ultra-high vacuum (UHV) conditions, where most surface science experiments are held.

In this work we consider a catalytic process, ethylene epoxidation, that has attracted considerable interest due to its large scale application in the chemical industry sector.[8] Oxidation of ethylene can lead to the formation of the desired product, ethylene oxide (EO), used for the synthesis of ethylene glycol, polyester fabrics, surfactants and detergents, or to total combustion, which proceeds through the formation of acetaldehyde (Ac). The common catalyst for this process is Ag supported on α-Al_2O_3, which, in the presence of suitable promoters such as Cs and Cl, can achieve a selectivity toward EO as high as 80%, while pure Ag leads to a selectivity of 40–50%.[9] Recent experiments and first-principles calculations by Linic *et al.* suggest that the formation of both EO and Ac on pure Ag proceeds through a common intermediate, an oxametallacycle (OMC) adsorbed on the Ag surface.[9,10] Moreover, the same authors suggested that alloying Ag with Cu increases the selectivity toward the formation of EO compared to pure Ag.[11,12] While the rationalization of the improved selectivity is to date based on the assumption of the formation of a two dimensional Ag–Cu surface alloy,[9,13,14] we have shown, through first-principles density functional theory (DFT) investigations[15–17] and through *in situ* X-ray photoelectron spectroscopy experiments,[17] that such a structure is not predicted to be stable in an oxygen–ethylene environment at temperatures and pressures relevant for industrial applications. Copper, on the other hand, segregates to the surface and forms stable thin oxide-like films.

Here, by means of DFT calculations, we study the reaction mechanism of ethylene epoxidation catalyzed by the thin oxide layers we predicted and found to be present at the surface of the Ag–Cu alloy under reaction conditions. We find that the mechanism of ethylene epoxidation is structure-dependent, and that the usual assumption of the formation of a common intermediate for both the selective and unselective path, while true for several surface structures, does not hold in general. These findings, in addition to providing new insights into this heterogeneous catalytic reaction, stress how the effects of temperature and pressure significantly impact the properties of catalysts and the reaction mechanisms they promote.

II. Methodology

We perform DFT calculations with the generalized gradient approximation (GGA-PBE) for the exchange and correlation potential,[18] using a planewave pseudopotential approach.[19] To model the alloy catalyst we use a periodically repeated slab geometry with adsorbates on one side of the slab. A 12 Å vacuum layer is used, which is found to be sufficient to ensure negligible coupling between periodic replicas of the slab. All the slabs we

[a]*DEMOCRITOS Simulation Center, CRN-IOM, Theory@Elettra Group, Trieste, Italy*
[b]*School of Physics, The University of Sydney, Sydney, New South Wales, 2006, Australia*
[c]*Scuola Internazionale Superiore di Studi Avanzati (SISSA), Via Bonomea 265, 34136 Trieste, Italy*
[d]*Fritz-Haber-Institut der Max-Planck-Gesellschaft, Faradayweg 4-6, D-14195 Berlin, Germany*
† This paper is part of a *Journal of Materials Chemistry* themed issue on Modelling of Materials. Guest editors: Julian Gale and Mark Wilson.

consider are 4 layers thick (3 Ag layers and 1 layer for the Cu/O adsorbates) and the bottom two layers of the slab are kept fixed in their bulk positions. While these slabs are admittedly thin, in the least favorable case, the very open (110) surface, increasing the thickness of the slab from 3 to 8 layers leads to changes in the adsorption energy of our test system (a full monolayer of oxygen on an Ag slab) of about 16 meV per O atom. Identical or thinner slabs have also been adopted in several other DFT studies of Ag structures.[13,14,20] The largest surface unit cell we consider is (4 × 4) on the (111) surface, while most of the structures investigated have a (2 × 2) unit cell. For all structures the **k**-point sampling is equivalent (or close) to a regular (12 × 12) uniform grid on the (1 × 1) unit cell of the (111) surface, and we use a smearing parameter of 0.03 Ry (0.41 eV). This choice gives adsorption energies of our test system converged within 1 meV. The kinetic energy cutoff for the planewave expansion is 27 Ry (200 Ry for the charge density), which gives adsorption energies for our test system converged within 8 meV. This computational setup has already been tested and employed in our previous publications.[15,16]

For the calculation of the reaction pathways we adopt the nudged elastic band (NEB) technique.[21] The transition state along the minimum energy path is located using the climbing image method.[21] In these calculations, to reduce the computational cost, we sample the Brillouin zone using a coarser **k**-point mesh, equivalent to a 6 × 6 × 1 mesh in the (1 × 1) surface unit cell of the (111) facet. All the atoms except the bottom two layers of the silver slab are allowed to relax during the NEB minimization, until the forces are less than 0.02 eV/Å. Keeping the geometry of the transition state fixed, its energy is then refined using the finer 12 × 12 × 1 **k**-point mesh. We have checked that this procedure results in errors in the transition state energy of less than 20 meV when compared to a NEB minimization carried out with the finer **k**-point mesh. All the calculations are performed using the PWscf code contained in the Quantum-ESPRESSO package.[19]

The NEB calculations reported in this work are performed on a set of surface structures that, in a series of publications by some of us,[15–17] were identified to yield the lowest surface free energy under conditions of temperature and oxygen partial pressure close to those found in industrial applications. Here we simply recall the theoretical approach used in those studies, namely the *ab initio* thermodynamics approach.[22] The structures are considered to be in thermodynamic equilibrium with an oxygen gas reservoir, described by its chemical potential. For each surface orientation, the most stable structures are the ones that minimize the surface free energy of adsorption:

$$\gamma(\mu_{Cu}, \mu_O) = (E_{tot} - E^{slab}_{Ag} - N_{Ag}\mu_{Ag} - N_{Cu}\mu_{Cu} - N_O\mu_O)/A \quad (1)$$

where E_{tot} is the total energy of the system, E^{slab}_{Ag} is the total energy of the 3 layer Ag slab, N_{Ag} is the number of Ag atoms in addition to the ones contained in the slab, N_{Cu} and N_O are number of Cu and O atoms, μ_{Ag}, μ_{Cu}, and μ_O are the chemical potential of Ag, Cu and O, respectively. Except for the oxygen reservoir, we neglect the vibrational and configurational entropy contributions, which allows us to identify the free energies with the total energies. The chemical potential of Ag is fixed at the value of bulk Ag, while we use the chemical potential of Cu as a parameter that controls the amount of Cu present in the particles. In the following we will measure the chemical potential of Cu with respect to its bulk value ($\Delta\mu_{Cu} = \mu_{Cu} - E^{bulk}_{Cu}$) and the chemical potential of O with the respect to half the energy of the oxygen molecule ($\Delta\mu_O = \mu_O - 1/2E^{tot}_{O_2}$). The chemical potential of oxygen can be directly linked to the temperature (T) and oxygen partial pressure (p_{O_2}).[22] At values of interest for practical applications ($T \sim 600$ K, $p_{O_2} \sim 1$ atm) we have $\Delta\mu_O = -0.61$ eV. Given the uncertainty connected to the precise determination of the O chemical potential due to the well known tendency of the PBE and similar functionals to overbind the oxygen molecule, we note that there is a significant error bar associated with the temperature and pressures determined through DFT calculations. In the case of the Ag–O system, Li *et al.*[23] estimated these error bars to be ~110 K for the determination of T and about three orders of magnitude for the oxygen partial pressure.

In Ref. 17 we also considered the stability of the surface oxide-like structures identified here when the reducing agent (ethylene, C_2H_4) is present in the gas atmosphere. To this end, we performed an analysis analogous to the one presented for the Ru–O system in Ref. 24, employing a "constrained thermodynamic equilibrium" approach. In the presence of a pure oxygen environment, the condition for the stability of the thin oxide layer structure (indicated here as $Ag_xCu_yO_z$) is:

$$g\mathrm{Ag}_x\mathrm{Cu}_y\mathrm{O}_z < x\mu_{Ag} + y\mu_{Cu} + z\mu_O \quad (2)$$

which leads to:

$$\begin{aligned}\Delta\mu_O &> \frac{1}{z}\left(g_{\mathrm{Ag}_x\mathrm{Cu}_y\mathrm{O}_z} - x\mu_{Ag} - y\mu_{Cu} - \frac{z}{2}E_{O_2}\right)\\ &\gtrsim \frac{1}{z}H_f(T = 0\ \mathrm{K}).\end{aligned} \quad (3)$$

Here $H_f(T = 0\ \mathrm{K})$ is the zero temperature formation energy of the $Ag_xCu_yO_z$ structure, and the approximation introduced is to neglect the temperature variation of this quantity, in line with the previous approximations where we neglected entropic contributions in solids.

If we now consider our system to be in thermodynamic equilibrium with an atmosphere containing only the reducing reactant, the condition of stability is:

$$g_{\mathrm{Ag}_x\mathrm{Cu}_y}\mathrm{O}_z + z\mu_{C_2H_4} < x\mu_{Ag} + y\mu_{Cu} + z\mu_{C_2H_4O(EO,Ac)}, \quad (4)$$

where the (EO,Ac) caption indicates that the condition of stability depends on which of the two products of the oxidation we consider. If we grossly approximate the chemical potential of the products of the oxidation with their internal energy in the gas phase, the condition of stability simplifies to:

$$\Delta\mu_{C_2H_4} < -\frac{1}{z}H_f(T = 0\ \mathrm{K}) + \Delta E^{mol}, \quad (5)$$

where $\Delta E^{mol} = E_{C_2H_4O(EO,Ac)} - E_{C_2H_4} - 1/2E_{O_2}$ is the difference in total energy between the three gas phase molecules. We compute this value to be −1.18 eV in the case of EO and −2.18 eV in the case of Ac.

If both oxygen and ethylene are present in the gas atmosphere, under "constrained equilibrium" conditions with the surface, the stability condition is obtained combining eqn (3) and (5):

$$\Delta\mu_{C_2H_4} - \Delta\mu_O \lesssim -\frac{2}{z}H_f(T = 0\ \mathrm{K}) + \Delta E^{mol}, \qquad (6)$$

while eqn (3) still applies for low C_2H_4 concentrations.

Using this approach we have shown that the most stable surface structures identified in an oxygen atmosphere are also stable in the presence of ethylene.[17] The range of stability of these surface structures is such that, under conditions of temperature and partial pressures of oxygen and ethylene, ethylene is not capable of reducing the oxide to form either EO or Ac. These findings are confirmed by the experimental evidence that XPS fingerprints of the formation of the thin surface oxides in an oxygen atmosphere are present also under reaction conditions, where ethylene is present.[17]

In Ref. 17 we also studied the equilibrium shape of the Ag–Cu particle in an oxygen environment. To this end we fixed the value of oxygen chemical potential at a value corresponding to $T = 600$ K and $p_{O_2} = 1$ atm) and used the Wulff construction[25] to determine the shape of the particle that minimizes its surface free energy as a function of the Cu chemical potential. We found that the relative areas of the low index facets can change substantially in a narrow range of μ_{Cu}, and that the (111) surface, at variance with the case of pure Ag, is not always the dominant facet.

III. Composition, surface structure and shape of the catalyst nanoparticles

In our previous publications we have already investigated the surface phase diagram of the Ag–Cu system in an oxygen atmosphere for the three low-index surface orientations as a function of oxygen chemical potential (*i.e.* T and p_{O_2}).[15–17] There we showed how, in the presence of oxygen in the atmosphere, the strength of the Cu–O interaction relative to that of Ag–O drives Cu to the surface. On the surface, Cu tends to form thin oxide-like layers, while surface alloys are not found to be stable.[15]

In Ref. 17 we studied the surface free energy of several candidate surface structures as a function of the Cu chemical potential, fixing the oxygen chemical potential corresponding to values of temperature and oxygen partial pressure typically used in experiments ($T = 600$ K and $p_{O_2} = 1$ atm). Given that X-ray photoemission spectroscopy (XPS) studies suggest that Cu is present on the surface in the (0.1–0.75) ML range,[12] we find that the values of the Cu chemical potential compatible with that coverage are those just around the formation of bulk copper oxide. We found that around the region of interest, both the (100) and (110) surfaces are covered with a one layer thin oxide-like structure with a 1 : 1 stoichiometry between Cu and O. We denote these thin-layer structures with the CuO label, even though they bear little to no resemblance to bulk CuO oxide. In the case of the (100) surface, Cu and O are arranged in a square lattice, with both elements 4-fold coordinated and a Cu–O distance of 2.08 Å. For the (110) surface, on the other hand, Cu and O are 2-fold coordinated, with Cu occupying "added row" positions on the underlying Ag surface. The Cu–O distance is, in this case, 1.81 Å. The (111) surface can be covered with either the p4-OCu_3 or the one layer thin CuO structure. The first is a (4 × 4) structure with ring-like O–Cu patterns and one OCu_3 unit removed. O atoms are coordinated to three Cu atoms and Cu atoms are coordinated to two O atoms, except around the missing unit, where the O coordination is reduced to two. In this case the Cu–O distance is around 1.84 Å. In the second structure O is coordinated to three Cu atoms and Cu is coordinated to either two or four oxygen atoms, and the Cu–O distances are between 1.82 and 1.95 Å. We also found that on the (111) surface there is a third surface structure with a surface free energy only slightly higher than the CuO and p4-OCu_3 structures. We label this structure p2, since it has a (2 × 2) periodicity. In this case each Cu atom is bonded with two O atoms and each O is coordinated to three Cu atoms, in a ring-like pattern. The relaxed geometries of the above mentioned structures are shown in Fig. 1.

An outcome of these calculations is that the two-dimensional Ag–Cu surface alloy is not stable in these conditions on any of the low-index facets. This is particularly relevant in view of the fact that the rationalization of the enhanced selectivity of the Ag–Cu alloy toward the formation of ethylene oxide compared to pure Ag was based on the assumption of the formation of a surface Ag–Cu alloy. Our theoretical and experimental study,[17] on the other hand, shows the formation of a thin copper oxide layer on the surface of the catalyst, suggesting that the formation of this material is the key to understand the superior performance of the Ag–Cu catalyst.

We stress here that catalytic systems are thermodynamic open systems, where reactants and products are continuously supplied and transported away. Under steady-state conditions, a variety of interdependent atomistic processes take place simultaneously at the surface of the catalyst. Recent experiments of the oxidation of CO on Pt(110) and Pd(100) performed in high temperature and high pressure conditions[26] have shown how, under steady-state conditions, thin oxides form at the surface and they continuously evolve in time. These considerations highlight the non-equilibrium nature of catalysis: the surface of a catalyst, due to the interplay of various atomistic processes, continuously evolves and fluctuates, implying that the structure and composition of the active material is likely to be different from the surface structures found in thermal equilibrium conditions. The theoretical analysis performed in this work under the assumption of thermal equilibrium clearly cannot capture the dynamical nature of heterogeneous catalysis, but gives a guideline to establish the relative stability of a set of candidate surface structures that could be relevant under catalytic conditions.

IV. Epoxidation reactions: mechanism and activation energies

Having determined the lowest free surface energy structures of the Ag–Cu catalyst in an oxygen atmosphere at temperatures and pressures of practical interest, we now consider the adsorption of ethylene and the two competing chemical reactions leading to the formation of Ac and EO. Ethylene is known to bind very weakly on clean Ag surfaces as well as on thin Ag oxide-like layers.[20,27] Here, as well, we find that the adsorption energy of ethylene never exceeds 0.15 eV on any of the surface structures considered. The location of the transition state (TS) is determined through the climbing-image NEB method using as the initial state the most stable configuration for ethylene adsorption and as the final state the product molecules in gas phase (*i.e.* far

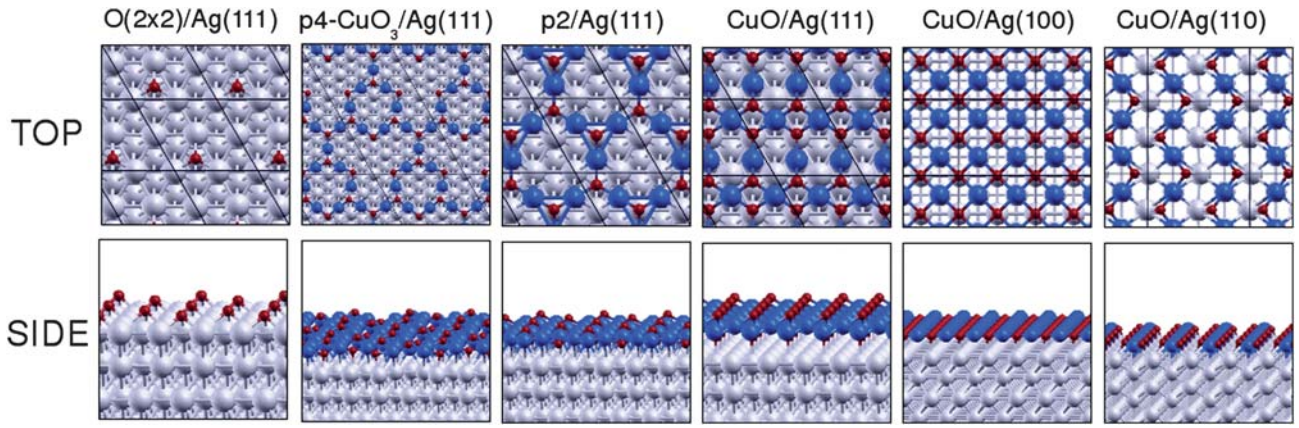

Fig. 1 Top and side view of the six low energy structures considered in this work. The small red atoms represent oxygen, the large blue ones represent copper and the grey represent silver.

enough from the surface so that they do not interact significantly with the surface).

On the Ag–O$^{(2\times2)}$(111) and Ag–O$^{(2\times2)}$(100) surface with pre-adsorbed oxygen both reactions are known to proceed through a common oxametallacycle (OMC) intermediate,[9,10,13,14] where ethylene is bonded with one C atom to a surface metal atom and with the other C atom to oxygen. The formation of Ac has a slightly (0.01 eV[9] to 0.07 eV[13]) smaller activation barrier in both cases, in agreement with experimental measurements.[9] Similar conclusions have been reached also for the thin Ag oxides.[28] We find, on the other hand, that on the thin copper-oxide layers the picture is different. We find that while the formation of Ac always proceeds from the formation of an intermediate (OMC occurs in all cases except for the p2 structures, where ethylenedioxy forms), the formation of EO can proceed through different paths, depending on the surface structure of the catalyst.

The formation of EO on the p2/Ag(111) and p4-OCu$_3$/Ag(111) structures does not involve the formation of an intermediate. In the case of CuO/Ag(111) we find that there are two competing reaction paths for the formation of EO. For the lowest energy one, EO is formed directly from the physisorbed ethylene molecule, without the formation of any intermediate. In the second path, whose transition state is only slightly (0.02 eV) higher in energy than the direct path, the reaction goes through the formation of an OMC.

We find that the OMC is a common intermediate for both the formation of Ac and EO in the case of Ag–O$^{(2\times2)}$/Ag(111), CuO/Ag(100) and CuO/Ag(110). These findings clearly stress how the reaction mechanism is structure-dependent.

The activation energies for the formation of Ac (E^*_{Ac}) and EO (E^*_{EO}) are shown in Table 1, together with their difference ($\Delta E^* = E^*_{Ac} - E^*_{EO}$). A positive value of ΔE^* suggests a selective formation of EO. In Fig. 2 we show the energy profile of the two competing reactions on some of the most relevant surface structures. The energies of the initial and final states correspond to the reagents and products physisorbed on the surface. There is a range of possible values for the activation barriers, due to the different mechanisms underlying the epoxidation reactions on different surface structures. In addition to the activation barriers reported in Table 1, we note that, using analogous methodologies to the ones employed here, the value of ΔE^* for the Ag–O$^{(2\times2)}$(100) surface has been found to be just 0.01 eV smaller that the one on the Ag–O$^{(2\times2)}$(111) structure.[14,29] We can see that all the Cu-containing structures provide a better selectivity toward EO compared to pure Ag structures, in agreement with the superior selectivity of Ag–Cu alloys compared to pure Ag seen in experiments.[9] The p2/Ag(111) structure, in particular, is very selective, although it involves activation energies larger that any other surface structure considered here. The structures on the (100) and (110) surfaces, on the other hand, provide only a marginally higher selectivity then the Cu-free structures.

For the case of the CuO/Ag(111) structure, since, in the lowest energy path, the formation of Ac proceeds through the formation of a metastable OMC while the formation of EO does not, determining an effective activation energy for the first process in order to directly compare the two reactions is difficult, since the population of the intermediate state under steady-state reaction conditions is not known. To this end we adopt the so-called "Sabatier analysis" proposed by Nørskov *et al.*,[30,31] which gives an estimate of the rate of a chemical process if all coverages are optimum for each elementary reaction step. Here we use the same notation and closely follow the analysis proposed in Ref. 31.

The elementary steps for our system, in the case of the CuO/Ag(111) structure, are the following:

$$C_2H_4 + {}^* \rightleftharpoons C_2H_4 \quad \text{(R1)}$$

$$O_2 + {}^* \rightleftharpoons O_2{}^* \quad \text{(R2)}$$

Table 1 Cu surface content (Θ_{Cu}), activation barriers for the formation of acetaldehyde (E^*_{Ac}) and ethylene oxide (E^*_{EO}) and the difference between the two (ΔE^*) for selected surface structures

Structure	Θ_{Cu}(ML)	ΔE^*(eV)	E^*_{Ac}(eV)	E^*_{EO}(eV)
O(2 × 2)/Ag(111)	0.00	–0.08	0.64	0.72
p4-OCu$_3$(111)	0.56	–0.04	1.04	1.08
p2(111)	0.75	0.45	1.94	1.49
CuO/Ag(111)	1.00	>0.02	>1.12	1.10
CuO/Ag(100)	1.00	0.02	0.94	0.92
CuO/Ag(110)	1.00	–0.06	0.90	0.96

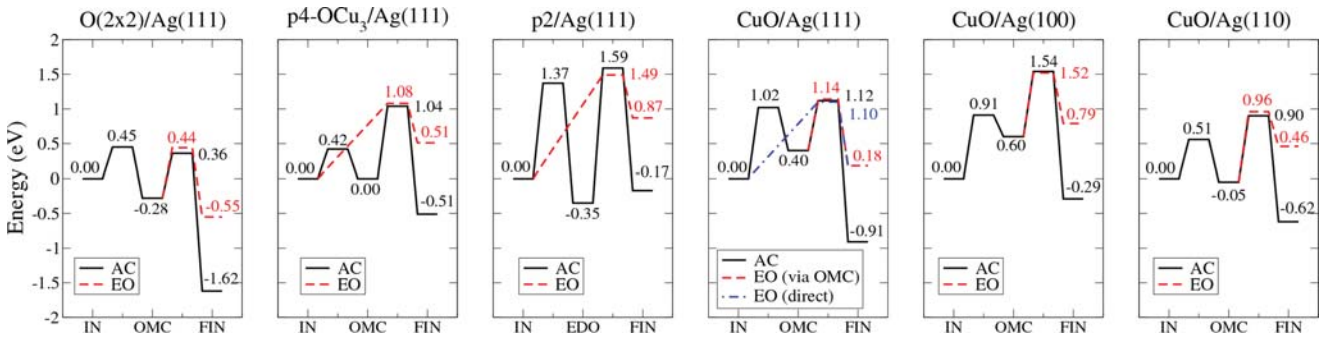

Fig. 2 Energy profiles for ethylene epoxidation over selected surface structures. At the initial state (IN) ethylene is physisorbed on the surface, the intermediate state is the oxametallacycle, while at the final state (FIN) the reaction has either produced acetaldehyde (Ac, black solid line) or ethylene oxide (EO, red dashed line). The energies of the final states correspond to the products physisorbed on the surface. The reaction can proceed through the formation of intermediates such as the oxametallacycle (OMC) or ethylenedioxy (EDO). The zero of energy is set at the initial state.

$$O_2 + 2^* \rightleftharpoons 2O^* \quad \text{(R3)}$$

$$C_2H_4 + O^* \rightleftharpoons OMC^* \quad \text{(R4)}$$

$$OMC^* \rightleftharpoons Ac + {}^* \quad \text{(R5)}$$

$$OMC^* \rightleftharpoons EO + {}^* \quad \text{(R6)}$$

where * indicates an empty site, while the same symbol next to a molecule indicates that the molecule is adsorbed on the surface. The forward and reverse rate constants of the reactions (R3)–(R6) are given by $k_i = \nu_i \exp[-\Delta G_i^*/kT] = \nu_i \exp[-(E_i^* - T\Delta S_i^*)/kT]$, where ν_i is a prefactor, E_i^* is the activation energy and k is the Boltzmann constant. ΔS_i^* is the entropy difference between the transition state and the initial state. The entropy of adsorbed species is assumed to be zero, and the gas-phase entropies are taken from Ref. 32. To maximize the rate for reactions (R3)–(R6) we neglect the reverse reactions:

$$r_3^+ = k_3^+ \Theta_{O_2} \Theta_* \quad (7)$$

$$r_4^+ = k_4^+ \Theta C_2H_4 \Theta_O \quad (8)$$

$$r_5^+ = k_5^+ \Theta OMC \quad (9)$$

$$r_6^+ = k_6^+ \Theta C_2H_4 \Theta_* \quad (10)$$

where, Θ_{O2}, Θ_O, ΘC_2H_4 and Θ_{OMC} are the coverage of adsorbed oxygen molecules, atomic oxygen, C_2H_4 and Θ_{OMC}, respectively. Θ_* is the coverage of empty sites on the surface. To find the optimum coverages, we first neglect the coverage of atomic oxygen and assume (R1) and (R2) to be in equilibrium:

$$\Theta_*^{max} = \frac{1}{1 + K_1 p_{C_2H_4} + K_2 p_{O_2}} \quad (11)$$

where K_1 and K_2 are the equilibrium constants for (R1) and (R2). The optimum coverages of C_2H_4 and O_2 have similar expressions, namely $\Theta^{max}{}_{C_2H_4} = K_1 p_{C_2H_4} \Theta_*$ and $\Theta_{O2}^{max} = K_2 p_{O_2} \Theta_*$. The optimum coverage of OMC can be found from $\Theta_{OMC} = K_4 \Theta_{C_2H_4} \Theta_O$, considering a full monolayer of adsorbed atomic oxygen and the maximum coverage for C_2H_4. The Sabatier rates are found by using the forward rates and the optimum coverages:

$$r_3^{Smax} = k_3^+ \Theta_{O2}^{max} \Theta_*^{max} \quad (12)$$

$$r_4^{Smax} = K_4^+ \Theta^{max}{}_{C_2H_4} \Theta_O^{max} = k_4^+ \Theta^{max}{}_{C_2H_4} \quad (13)$$

$$r_5^{Smax} = k_5^+ \Theta_{OMC}^{max} \quad (14)$$

$$r_6^{Smax} = k_6^+ \Theta^{max}{}_{C_2H_4} \Theta_*^{max} \quad (15)$$

The Sabatier rate for the formation of EO is given by the lowest of the Sabatier rates of reactions (R3) and (R6), while in the case of the formation of Ac we have to consider the slowest reaction among (R3), (R4) and (R5):

$$r^S{}_{EO} = \min(2r_3{}^{Smax}, r_6{}^{Smax}) \quad (16)$$

$$r^S{}_{Ac} = \min(2r_3{}^{Smax}, r_4{}^{Smax}, r_5{}^{Smax}). \quad (17)$$

To extract the difference in the effective activation energy of the two competing processes, we take all the prefactors ν_i to be identical and assume an Arrhenius type law for both processes. We therefore have:

$$r_{EO}^S = \nu \exp(-E_{EO}^*/kT) \quad (18)$$

$$r_{Ac}^S = \nu \exp(-E_{Ac}^*/kT) \quad (19)$$

$$\Delta E^* = E_{Ac}^* - E_{EO}^* = kT \ln(r_{EO}^S/r_{Ac}^S) \quad (20)$$

Not surprisingly, since we have assumed that reactions (R1) and (R2) are in equilibrium, the difference in the effective activation energy of the two competing processes is 0.02 eV, exactly the difference between the highest points in the energy profiles of the two processes, as can be seen in Fig. 2. This, however, is a lower bound for this difference, since the high activation energy for the formation of OMC will likely prevent this intermediate from having the optimal coverage. An upper bound can be obtained by considering reaction (R5) to be in equilibrium. Repeating the same reasoning outlined above we obtain a much larger 1.01 eV difference in the effective activation energies. Therefore, depending on the details of the kinetics of the two competing processes, this surface structure can be slightly to very selective toward the formation of EO.

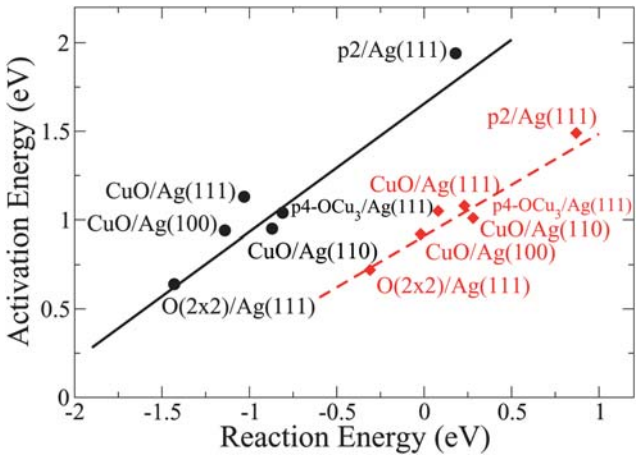

Fig. 3 Brønsted–Evans–Polanyi relation between the reaction energy and the activation energy. The black circles correspond to the formation of acetaldehyde, while the red diamonds correspond to the formation of ethylene oxide. The solid line and the red dashed line are linear fits for the formation of acetaldehyde and ethylene oxide, respectively.

In agreement with previous investigations,[14] we find that the activation energy and the reaction enthalpy are approximately related by a Brønsted–Evans–Polanyi (BEP) relation.[33–35] As we can see from Fig. 3, the two reactions, though, display a different dependence of the activation energy on the reaction enthalpy. This is at variance with the universal relation proposed for the dissociation reaction of simple molecules on different metal surfaces. [36] Here the two reactions involve different mechanisms (hydrogen shift between the two C atoms and formation of a C=O double bond in the Ac case, closure of the epoxy ring in the case of EO) and thus display a different BEP law. Interestingly, we find that the geometry of the two transition states is only weakly influenced by the underlying surface structure. As shown in Fig. 4, the reactions on all the surfaces considered share very similar TS's. Based on the assumption of the presence of the OMC intermediate, Kokalj *et al.*[14] described the formation of the TS for Ac as a partial break of both the bond between O and the surface and the one between C and the surface, whereas in the formation of EO at the TS the bond between C and the surface is completely cleaved. This interpretation suggests that the difference between the C- and O-surface binding energy is the appropriate descriptor to explain the enhanced selectivity of Cu-containing structure, such as the surface alloy.[14] Here we have shown, though, that the OMC is not always an intermediate and that an enhancement in selectivity of some surface structures can be attributed to a structure-dependent mechanism that has no resemblance to the clean Ag or 2D surface alloy case.

The results presented in this work suggest, therefore, that there is not a unique surface structure that is solely responsible for the catalytic activity of the Ag–Cu alloy. We have shown that in an oxidizing atmosphere a variety of surface structures can be present, and that there is not a unique mechanism for ethylene oxidation that applies to all stable structures. Several of these structures present similar activation barriers toward the formation of the oxidation products and are therefore likely to play

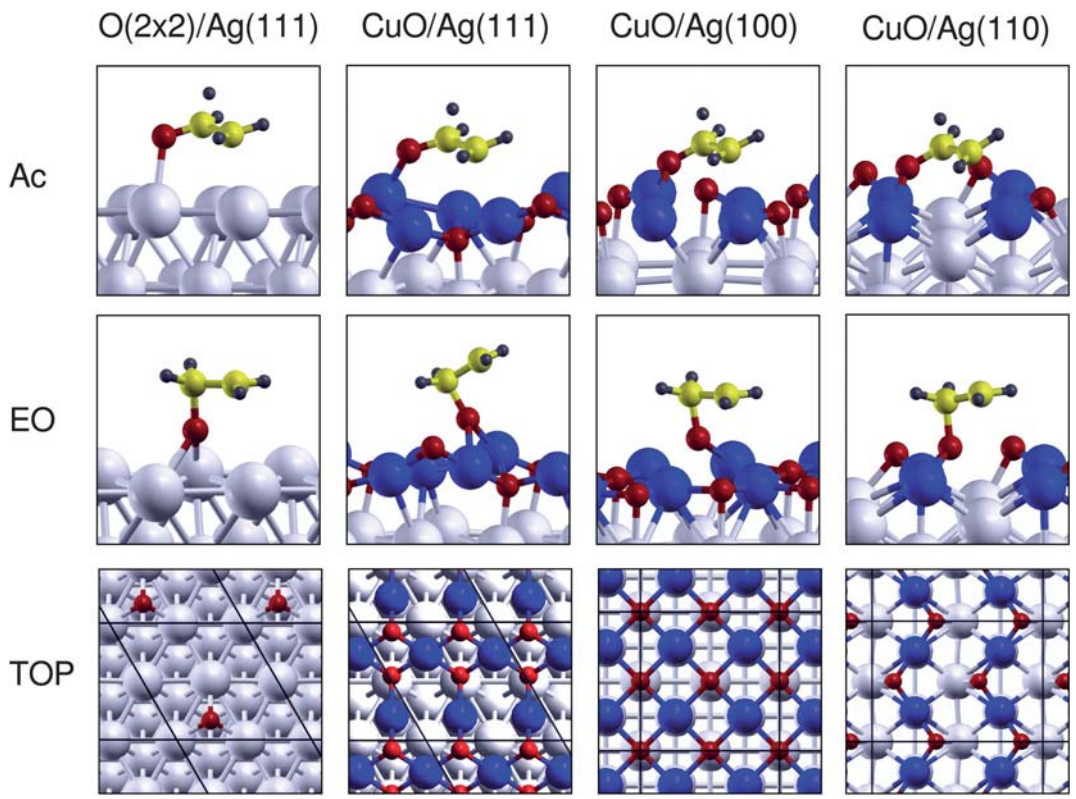

Fig. 4 Sketch of the transition state geometries for the formation of acetaldehyde (top panels) and ethylene oxide (central panels) and top view of the surface for four structures. The large gray light spheres represent Ag atoms, the large blue dark ones Cu, the medium red ones O and the small gray ones H. Note how the geometry of the transition state is, to a large degree, independent of the surface structure.

a role in the catalytic process. In this picture, the synergetic interplay of different reaction pathways and of different surface structures is crucial for describing and understanding the efficiency and long time-scale catalysis of the steady state. The temporal fluctuations of the local structure and composition among the ones identified in this work, and the resulting change in the mechanism of reaction, determine what we refer to as the "system chemistry" of the Ag–Cu alloy, which extends the "one-structure, one-mechanism" picture often assumed in heterogeneous catalysis.

V. Conclusions

In summary, we have investigated the mechanism of ethylene epoxidation catalyzed by the Ag–Cu alloy. This material, in an oxygen atmosphere, forms thin copper oxide layers on top of silver. These structures are stable against reduction by ethylene under reaction conditions, as predicted theoretically and confirmed experimentally.[17] Depending on the facet and the conditions of temperature and oxygen partial pressure, several surface structures can form. Here we studied how the reactions that convert ethylene to ethylene oxide and acetaldehyde proceed on each of the stable surface structures. We find that the reaction mechanism of ethylene epoxidation is influenced by the underlying surface structures, and that the reactions now always proceed through the formation of an oxametallacycle intermediate. We also find that the geometry of the transition states is not very sensitive to the surface structure and that activation barriers and enthalpies of reaction are approximately related by the linear Brønsted–Evans–Polanyi relation. The DFT estimates of the activation barriers for the competing processes suggest that these thin Cu–O layers can enhance the selectivity toward the formation of EO, even though our calculations suggest that the improvement in the selectivity is small.

Reference

1 B. Hodnett, *Heterogeneous Catalytic Oxidation*, John Wiley and Sons Ltd., Chichester, UK, 2000.
2 V. Johanek, M. Laurin, A. W. Grant, B. Kasemo, C. R. Henry and J. Libuda, *Science*, 2004, **304**, 1639.
3 F. Silly and M. R. Castell, *Phys. Rev. Lett.*, 2005, **94**, 046103.
4 F. Mittendorfer, N. Seriani, O. Dubay and G. Kresse, *Phys. Rev. B: Condens. Matter Mater. Phys.*, 2007, **76**, 233413.
5 P. Nolte, A. Stierle, N. Y. Jin-Phillipp, N. Kasper, T. U. Schulli and H. Dosch, *Phys. Chem. Chem. Phys.*, 2000, **2**, 3473.
6 K. Reuter, C. Stampfl and M. Scheffler, in *Handbook of Materials Modeling*, ed. S. Yip, Springer, Berlin, Heidelberg, 2005, chapter: Ab initio atomistic thermodynamics and statistical mechanics of surface properties and functions.
7 N. Seriani and F. Mittendorfer, *J. Phys.: Condens. Matter*, 2008, **20**, 184023.
8 *Chem. Eng. News*, 2001, **77**, 19.
9 S. Linic and M. A. Barteau, *J. Am. Chem. Soc.*, 2003, **125**, 4034.
10 S. Linic and M. A. Barteau, *J. Am. Chem. Soc.*, 2002, **124**, 310–317.
11 S. Linic, J. Jankowiak and M. A. Barteau, *J. Catal.*, 2004, **224**, 489.
12 J. T. Jankowiak and M. A. Barteau, *J. Catal.*, 2005, **236**, 366.
13 D. Torres, N. Lopez, F. Illas and R. Lambert, *J. Am. Chem. Soc.*, 2005, **127**, 10774.
14 A. Kokalj, P. Gava, S. de Gironcoli and S. Baroni, *J. Catal.*, 2008, **254**, 304.
15 S. Piccinin, C. Stampfl and M. Scheffler, *Phys. Rev. B: Condens. Matter Mater. Phys.*, 2008, **77**, 075426.
16 S. Piccinin, C. Stampfl and M. Scheffler, *Surf. Sci.*, 2009, **603**, 1467.
17 S. Piccinin, S. Zafeiratos, C. Stampfl, T. Hansen, M. Havecker, D. Teschner, V. Bukhtiyarov, F. Girgsdies, A. Knop-Gericke, R. Schlögl and M. Scheffler, *Phys. Rev. Lett.*, 2010, **104**, 035503.
18 J. P. Perdew, K. Burke and M. Ernzerhof, *Phys. Rev. Lett.*, 1996, **77**, 3865.
19 P. Giannozzi, S. Baroni, N. Bonini, M. Calandra, R. Car, C. Cavazzoni, D. Ceresoli, G. L. Chiarotti, M. Cococcioni, I. Dabo, A. D. Corso, S. de M Gironcoli, S. Fabris, G. Fratesi, R. Gebauer, U. Gerstmann, C. Gougoussis, A. Kokalj, M. Lazzeri, L. Martin-Samos, N. Marzari, F. Mauri, R. Mazzarello, S. Paolini, A. Pasquarello, L. Paulatto, C. Sbraccia, S. Scandolo, G. Sclauzero, A. P. Seitsonen, A. Smogunov, P. Umari and R. M. Wentzcovitch, *J. Phys.: Condens. Matter*, 2009, **21**, 395502, URL http://stacks.iop.org/0953-8984/21/i=39/a=395502.
20 F. Bocquet, P. Sautet, J. Cerda, C. Carlisle, M. Webb and D. King, *J. Am. Chem. Soc.*, 2003, **125**, 3119.
21 G. Henkelman, B. Uberuaga and H. Johnson, *J. Chem. Phys.*, 2000, **113**, 9901.
22 K. Reuter and M. Scheffler, *Phys. Rev. B: Condens. Matter Mater. Phys.*, 2001, **65**, 035406.
23 W.-X. Li, C. Stampfl and M. Scheffler, *Phys. Rev. B: Condens. Matter Mater. Phys.*, 2003, **67**, 045408.
24 K. Reuter and M. Scheffler, *Appl. Phys. A: Mater. Sci. Process.*, 2004, **78**, 793.
25 G. Wulff, *Z. Krist.*, 1901, **34**, 449.
26 B. L. M. Hendriksen, S. C. Bobaru and J. W. M. Frenkel, *Top. Catal.*, 2005, **36**, 43.
27 A. Kokalj, A. D. Corso, S. D. Gironcoli and S. Baroni, *J. Phys. Chem. B*, 2002, **106**, 9839.
28 F. Bocquet and D. Loffreda, *J. Am. Chem. Soc.*, 2005, **127**, 17207.
29 P. Gava, PhD thesis, SISSA, 2005.
30 T. Bligaard, J. Nørskov, S. Dahl, J. Matthiesen, C. Christensen and J. Sehested, *J. Catal.*, 2004, **224**, 206.
31 H. Falsig, B. Hvolbaek, I. S. Kristensen, T. Jiang, T. Bligaard, C. H. Christensen and J. K. Nørskov, *Angew. Chem., Int. Ed.*, 2008, **47**, 4835.
32 *CRC Handbook of Chemistry and Physics*, CRC Press, Boca Raton, FL, 1995.
33 N. Brønsted, *Chem. Rev.*, 1928, **5**, 231.
34 M. G. Evans and N. P. Polanyi, *Trans. Faraday Soc.*, 1938, **34**, 11.
35 A. Logadottir, T. H. Rod, J. K. Nørskov, B. Hammer, S. Dahl and C. J. H. Jacobsen, *J. Catal.*, 2001, **197**, 229–231.
36 J. K. Nørskov, T. Bligaard, A. Logadottir, S. Bahn, L. B. Hansen, M. Bollinger, H. Bengaard, B. Hammer, Z. Sljivancanin, M. Mavrikakis, Y. Xu, S. Dahl and C. J. H. Jacobsen, *J. Catal.*, 2002, **209**, 275.